



# Development of a novel cost effective methanol electrolyzer stack with Pt-catalyzed membrane



Sundar Pethaiah Sethu<sup>a,c,\*</sup>, Sasikumar Gangadharan<sup>b</sup>, Siew Hwa Chan<sup>c</sup>, Ulrich Stimming<sup>a</sup>

<sup>a</sup>TUM CREATE, 1 CREATE Way, #10-02 CREATE Tower, Singapore 138602, Singapore

<sup>b</sup>Agni College of Technology, Chennai 603 103, Tamil Nadu, India

<sup>c</sup>Energy Research Institute @NTU, Nanyang Technological University, 50 Nanyang Drive, Singapore 637553, Singapore

## HIGHLIGHTS

- Developed electrolyzer system produces 102 L h<sup>−1</sup> of 99% pure hydrogen without CO.
- Catalyzed membrane is prepared by non-equilibrium impregnation-reduction method.
- Catalyzed membrane shows better performances than normal membrane.
- Methanol electrolysis consumes 1.89 kWh Nm<sup>−3</sup> H<sub>2</sub> which is less than water electrolysis.

## ARTICLE INFO

### Article history:

Received 21 October 2013

Received in revised form

18 December 2013

Accepted 19 December 2013

Available online 1 January 2014

### Keywords:

Fuel cell

Impregnation reduction method

Catalyzed membrane

Hydrogen

Methanol

Electrolysis

## ABSTRACT

This paper demonstrates a novel polymer electrolyte membrane (PEM) based methanol electrolyzer stack with a catalyzed membrane for hydrogen production. The physical and electrochemical properties of the catalyzed membrane, single cell and stack are examined using various characterization techniques, such as X-ray diffraction, scanning electron microscopy with EDX and polarization studies. The results demonstrate that the with Pt-catalyzed membrane electrode assembly (MEA) exhibits significantly better performance than a normal MEA. The developed electrolyzer stack produces 102 L h<sup>−1</sup> of 99% pure hydrogen without CO and CO<sub>2</sub>. The excellent stability of the PEM methanol electrolyzer system is demonstrated by running the stack for 2500 h of intermittent operation with constant current density.

© 2013 Elsevier B.V. All rights reserved.

## 1. Introduction

Increasing environmental concern and rising fossil fuel cost due to increasing global energy demand have increased the urgency to look for alternative fuels that are clean and renewable. Among others, hydrogen, used in fuel cell technology, is considered as one of the most promising alternative fuel [1]. One particular area where fuel cell technology, specifically the polymer electrolyte membrane fuel cell (PEMFC) system, is gaining a lot of interest in the portable application, particularly in the automotive sector. However, in such applications, storage and distribution of hydrogen

pose a substantial challenge to the wider market acceptance of the technology. One of the most promising methods to overcome this challenge is to produce hydrogen on-site from a hydrogen-rich liquid fuel, such as ethanol or methanol, this solves both the storage and the distribution issues like existing fuels.

In general, alcohols can be used in fuel cells either directly as in the case of direct methanol fuel cell (DMFC) and direct ethanol fuel cell (DEFC) or indirectly to produce hydrogen by incorporating electrolyzer or reformer. However, both direct alcohol fuel cells and the reformer methods are not very efficient and they tend to have CO control issues [2–4]. To address all the above issues electrolysis of aqueous alcohol is a promising method for on-site hydrogen production with very high purity, and it has been reported that hydrogen can be generated by electrolysis of methanol–water mixtures at a lower operating voltage, compared to water electrolysis [5]. The electrochemical reaction at the anode, cathode and overall reaction is represented as follows:

\* Corresponding author. TUM CREATE, 1 CREATE Way, #10-02 CREATE Tower, Singapore 138602, Singapore. Tel.: +65 65923013; fax: +65 68969950.

E-mail addresses: [sundar.pethaiah@tum-create.edu.sg](mailto:sundar.pethaiah@tum-create.edu.sg) (S.P. Sethu), [ulrich.stimming@tum-create.edu.sg](mailto:ulrich.stimming@tum-create.edu.sg) (U. Stimming).

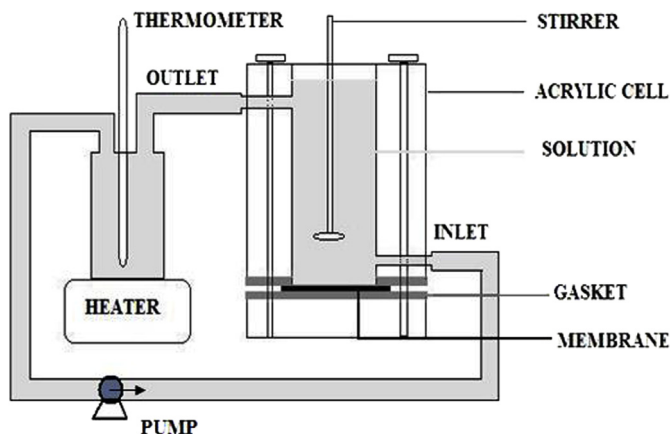
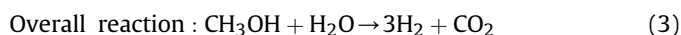
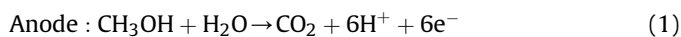


Fig. 1. Cross sectional view of the experimental setup.



It is widely reported that the Pt-catalyzed membrane is suitable for electrolyzer applications [6–9]. In addition, the use of a Pt-catalyzed membrane as the anode for methanol oxidation offers advantages over conventional cells [6]. The first is related to the reported decrease in catalyst poisoning in a Nafion environment. Katayama et al. [7] reported that by using Pt bonded onto a Nafion PEM, a higher steady-state catalytic activity for methanol oxidation is resulted as compared to that from a Pt–Pt electrode. These attributed the improvement to the surface-mediator action of Pt (0) and Pt (II) in the oxidation of adsorbates. The PEM matrix was postulated to stabilize Pt (II). Another advantage of using a Pt-PEM electrode is that gaseous reactants can contact the electrode without dissolving into a liquid electrolyte which might cause mass-transfer limitations and may favor undesired side reactions. Moreover, a Pt-catalyzed membrane is durable during the vigorous gas evolution due to its adhesive property and porous structure. This decreases the risk of electrodes peeling due to the swelling of the PEM on absorbing methanol [8]. Catalyzed membrane preparation is also attractive as it involves only one step for the catalyst preparation and application processes.

Furthermore, the development of a catalyzed membrane by the non-equilibrium impregnation-reduction (NEIR) method is one of

the best methods for electrolyzer applications [9]. However, to the best of our understanding, no work has been reported on the performance of a platinum catalyzed membrane by NEIR method for methanol electrolyzer applications. Hence, in the present work the possibilities of a Pt-PEM electrode prepared by the NEIR method for methanol electrolyzer application have been investigated.

## 2. Experimental procedure

Proton exchange membrane (Nafion 117 DuPont) and high-purity chemicals such as Pt (NH<sub>3</sub>)<sub>4</sub> Cl<sub>2</sub> (Johnson Matthey), NaBH<sub>4</sub> (Merck), H<sub>2</sub>SO<sub>4</sub> (Merck), Carbon power (Cabot corporation), 40% Pt/C (Duralyst, USA), Nafion ionomer (Dupont), carbon cloth (Ballard) and CH<sub>3</sub>OH (Merck) were used in this work.

### 2.1. Membrane pre-treatment

The membrane was treated using the standard procedure in 5 wt.% H<sub>2</sub>O<sub>2</sub>, distilled water, 0.5 M H<sub>2</sub>SO<sub>4</sub> solution and finally de-ionized water, respectively for each 30 min at 80 °C [10]. The obtained membrane from the above treatments was dried for 12 h under vacuum oven at a constant temperature of 80 °C. The initial weight of the treated membrane was determined to find out the amount of Pt loading on the membrane surface [11]. After weighing the membrane, it was treated with 0.5 M NaCl to convert the membrane into Na<sup>+</sup> form. This is due to the water and methanol permeability in the acid form of the membrane is lower than that in its Na<sup>+</sup> forms, so this Na<sup>+</sup> form of the membrane will speed up the exchange process [12].

### 2.2. Preparation of catalyzed membrane

The platinum catalyzed membrane was prepared from NEIR method. The modified experimental set-up used in the present study is shown in Fig. 1. The top surface of the membrane was placed to face the impregnation solution of 0.6 mM Pt (NH<sub>3</sub>)<sub>4</sub> Cl<sub>2</sub> in methanol–water (1:3) mixture for about 50 min. After impregnation, the platinum solution was removed from the cell and replaced by the reducing agent of 10 mM NaBH<sub>4</sub> at pH 13 for 2 h. The solution was continuously stirred at 190 rpm and the temperature was maintained at 50 °C. Finally, reduced Pt on membrane was soaked in a 0.5 M H<sub>2</sub>SO<sub>4</sub> solution followed by de-ionized water treatment for 1 h at 80 °C and then dried using vacuum heating oven. The membrane was weighed again and measured the final weight of the amount of Pt loading. The similar technique was employed to the other side of the catalyzed membrane. The Pt loading on the membrane was controlled by impregnation time. Finally, the Pt/PEM/Pt was soaked in 0.5 M H<sub>2</sub>SO<sub>4</sub> and de-ionized water for 1 h and weighed followed by complete drying. The resulting amount of Pt loading was 0.5 and 1 mg cm<sup>−2</sup> for cathode and anode respectively. The initial and final concentrations of Pt in the impregnation solution were estimated gravimetrically which supported the amount of catalyst loading on the membrane surface. The active area of the electrode was 50 cm<sup>2</sup>. For comparative evaluation a normal MEA with 40% Pt/C was prepared based on our prior study [5]. All the other parameters were kept constant to facilitate the comparative study.

### 2.3. Single cell and stack assembly

Single cell experiments were performed by placing the Pt-catalyzed membrane between two silicone rubber gaskets of thickness 0.25 mm and inserted between two graphite plates with straight parallel grooves and 50 cm<sup>2</sup> active areas (Fig. 2). A gas diffusion layer (GDL) with novel pore design (Fig. 3) was placed on both sides of the Pt-catalyzed membrane for effective current

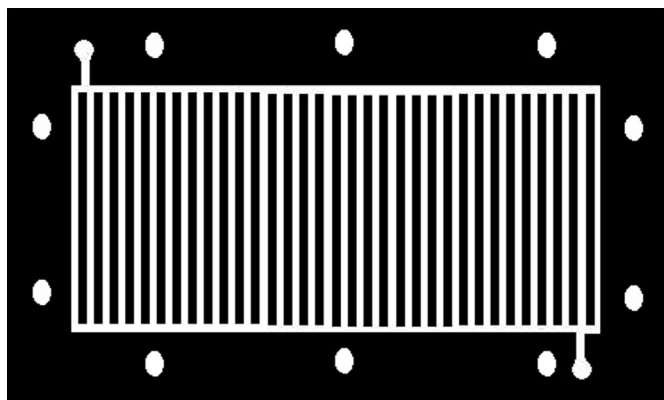


Fig. 2. Graphite plates with straight parallel grooves.

distribution and gas evolution. The above items were clamped together using nuts and bolts, by applying uniform torque, to assemble the single cell. The cell had provision for heating, temperature control and had suitable ports for feeding the reactants and removal of products. For comparative study a normal MEA single cell also assembled with same above setup.

The electrolyzer stack was built placing the Pt-catalyzed membranes inside the bipolar graphite plates. The MEAs were assembled into the 5-cell arrangement between four bipolar plates, two current collectors made from a silver-plated copper steel sheet were positioned at each end of the stack. Silicone rubber gaskets were placed between bipolar plates to prevent gas leakage to the exterior and inside the stack. Parallel type flow fields were machined in 4 mm thick graphite plates. The stack assembly including the MEAs, gaskets, bipolar plates, and current collectors was clamped between two end plates made with hylam sheet by twelve bolts. The overall specification of the methanol electrolyzer stack is given in Table 1.

#### 2.4. Electrolyzer system configuration

PEM methanol electrolyzer system comprises of an electrolyzer stack, MeOH/water reservoir, pump to feed the fuel (methanol–water mixture) to the anode of the electrolyzer stack, thermocouple to maintain the stack temperature, MeOH level indicator, regulated DC power supply to enable the electrochemical reaction to occur by applying a constant voltage, hydrogen sensor and mass flow meter, silica gel desiccant, de-humidifier and hydrogen gas relative humidity monitor. There is a master electronic control unit with display configured to control the stack voltage, temperature, dehumidifier, pump speed, H<sub>2</sub> sensor, solenoidal and isolation valve operation. Hydrogen gas sensor/monitors are placed immediately after the silica desiccant to measure the purity and flow of the generated H<sub>2</sub> gases so as to evaluate the compatibility to feed to the fuel cell. At the anode side, the unutilized MeOH fuel is fed back to the reservoir and CO<sub>2</sub> is vented out. The electrolysis was conducted to the electrolytic cell using a DC power supply. The overall process flow diagram is schematically represented in Fig. 4.

#### 2.5. Physical characterizations

X-ray diffraction (XRD) pattern of Pt coated Nafion membrane is acquired at room temperature with X'pert PRO PANalytical diffractometer using Cu-K $\alpha$  radiation as source and operated at 40 kV. The sample was scanned in the 2 $\theta$  ranging from 10 to 80° for 2 s in the step scan mode. Surface morphology, cross sectional and the EDX of the Pt catalyzed membrane were depicted using FESEM at 10 keV (JEOL-6340F).

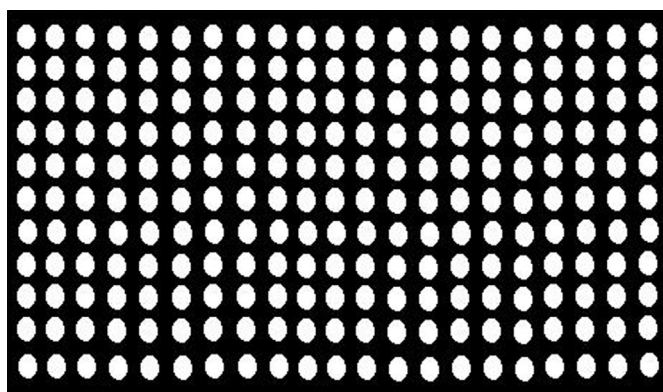


Fig. 3. Gas diffusion layer with novel pore design.

Table 1

Overall specification of the methanol electrolyzer stack nominal.

Parameter	Specification
Number of cell	5
Electrode area	50 cm <sup>2</sup>
Electrolyte	Nafion® 117
Catalyst	Platinum
Current collectors	Carbon cloth (gas diffusion layer)
Flow field plate	Graphite plates with straight parallel grooves
Nominal H <sub>2</sub> production rate	102 L h <sup>-1</sup>
Nominal current and voltage	50 A at 3.95 V

#### 2.6. Electrochemical characterizations

Cyclic voltammetry (CV) technique was used to measure the roughness factor of the electrolyzer electrodes. Pure argon and hydrogen gas were passed through the working electrode (cathode) and reference electrode (anode) compartments, respectively. Using an electrochemical analyzer (Auto lab), the potential was swept between 0 and 1.2 V vs. RHE at a scan rate of 15 mV s<sup>-1</sup>. The anode serves as both the reference and counter-electrode. From the CV, the charge equivalent to the area under the hydrogen desorption region was evaluated which is useful to calculate the roughness factor and electroactive surface area [13,14]. We assumed that the charge required for the adsorption/desorption of a monolayer of atomic hydrogen on the surface is about 210  $\mu\text{C cm}^{-2}$ .

The electrolysis was conducted to generate hydrogen at the cathode, by applying current across the two terminals of the electrolyzer using a programmable DC power supply unit having constant current and voltage mode provisions. Hydrogen production rate was calculated from the cell current and was cross examined by gas volume measurement. Purity of hydrogen gas was checked by calibrated hydrogen purity analyzer (NOVA Gas Analyzer). In order to find out about the stability, long time performance was studied at constant current density.

### 3. Results and discussions

#### 3.1. Physical characterization of catalyzed membrane

Fig. 5 shows the X-ray diffraction patterns of Nafion 117 membrane and Pt-catalyzed Nafion 117 membrane respectively. The first peak located at about 16.5° in the both XRD patterns is associated to the crystalline peak of Nafion® [15]. The other peaks corresponding to the lattice planes (1 1 1), (2 0 0) and (2 2 0) of Pt are observed at 2 $\theta$  = 40°, 46°, 67° for Pt-catalyzed membrane. Which confirms the fcc cubic structure of Pt. These values are well correlated with the JCPDS (JCPDS: 882343) data. The particle size of Pt in sample is calculated using Debye-Scherrer's relation [14].

$$D = \frac{0.94\lambda}{\beta \cos \theta} \quad (4)$$

Here,  $\lambda$  is wavelength of incident X-ray,  $\beta$  is full width half maximum and  $\theta$  is diffraction angle. The calculated average particle size of Pt coated on the membrane surface is 5.2 nm. The particle size of the Pt catalyzed membrane is slightly bigger than that of commercial 40% Pt/C catalyst (Duralyst, USA), equal to 3 nm from XRD measurements (not shown). It can be easily explained by the different preparation conditions of the catalyst samples in both cases [16].

The cross sectional image and surface morphology of Pt-catalyzed membrane is shown in Fig. 6a and b respectively. From the HRSEM analysis, the membrane forms a Pt deposit in the interface region and intimate contact with membrane (Fig. 6a),

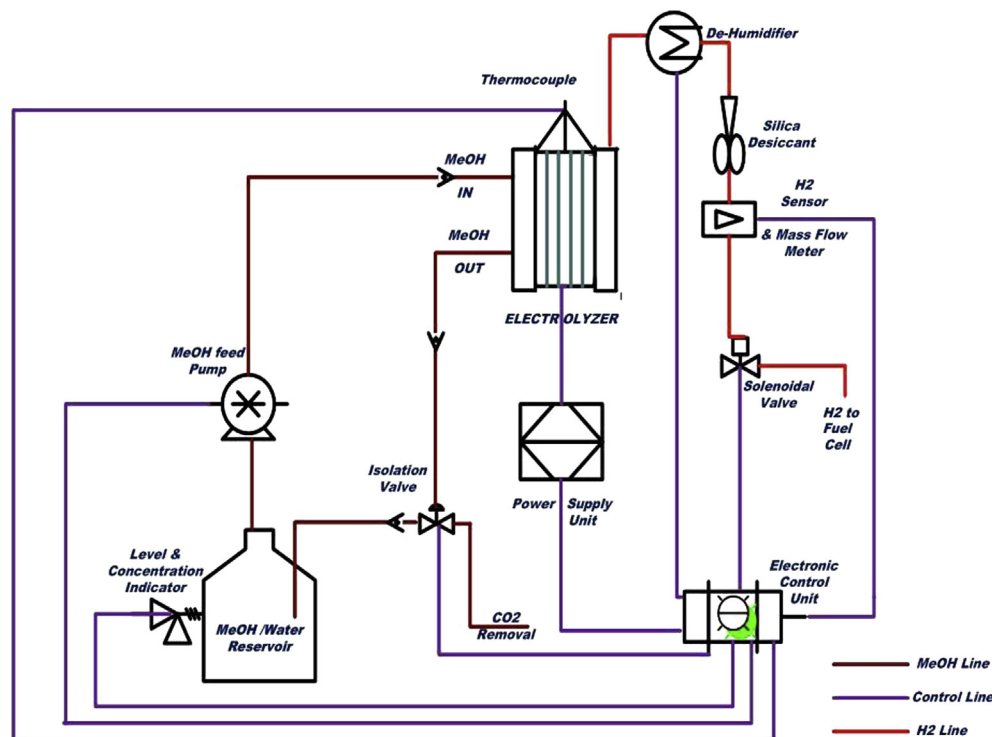


Fig. 4. Flow diagram of the system.

moreover the Pt particles exist uniformly in the membrane with porous structure (Fig. 6b). It facilitates the methanol oxidation and gas evolution. The EDX image of Pt-catalyzed membrane is shown in the Fig. 7, which also confirms the presence of Pt on membrane.

### 3.2. Electrochemical characterizations of methanol electrolyzer

#### 3.2.1. Cyclic voltammetry studies

Fig. 8 shows the CV of Pt-catalyzed MEA and normal MEA. It has been recorded after 100 cycles to establish the reproducibility. During the first 100 cycles, the electrode has been scanned at  $100 \text{ mV s}^{-1}$ . The peak from 0 to 0.4 V provides information on the hydrogen adsorption and desorption which occurred on the platinum surface and from 0.4 to 0.5 V is considered as double layer

region. The roughness factor and electroactive surface area were calculated from the current densities of absorption and desorption and were integrated separately and referred to a charge of  $210 \mu\text{C cm}^{-2}$ , which was correlated to a monolayer of hydrogen absorption on the platinum surface [17].

Fig. 8 shows that the cell made from Pt-catalyzed MEA exhibits significantly larger hydrogen desorption peak than the normal MEA. As a result Pt-catalyzed MEA has higher electroactive surface area and roughness factor than the MEA prepared by the normal method; this may be due to the extension of the three-phase boundary in the catalyst layer [13,18] which leads to a better cell performance. The electrochemical properties of both MEAs are given in Table 2.

#### 3.2.2. Evaluation of methanol electrolyzer

It is well known that the power required for electrolysis is directly related to the applied cell voltage and current. Hence the electrolyzer performance was evaluated at various voltages by measuring the current density and hydrogen production rate. Initially, titanium (Ti) plate and Ti mesh were used for the fabrication of PEM methanol electrolyzer, because it was used in water electrolyzer. Since a methanol electrolyzer works at much lower cell voltage, it is fabricated by using graphite plates and novel pore designed GDL with a view to reduce the capital cost.

The methanol electrolyzer system with single cell and three cell stack was operated at  $80^\circ\text{C}$  using 4 M methanol [5]. The performance of the single cell is shown in Figs. 9 and 10. From the result it is observed that the Pt-catalyzed MEA exhibited better performance than the normal MEA, in particularly high current density region the difference is higher. This behavior could be explained by the effect of the electrode structure. The particular structure of the catalyzed membrane could result in higher catalyst utilization with respect to the normal ones, as previously suggested in the literature for different systems [19]. The uniform distribution and its intimate contact with Nafion membrane of platinum in the catalyzed

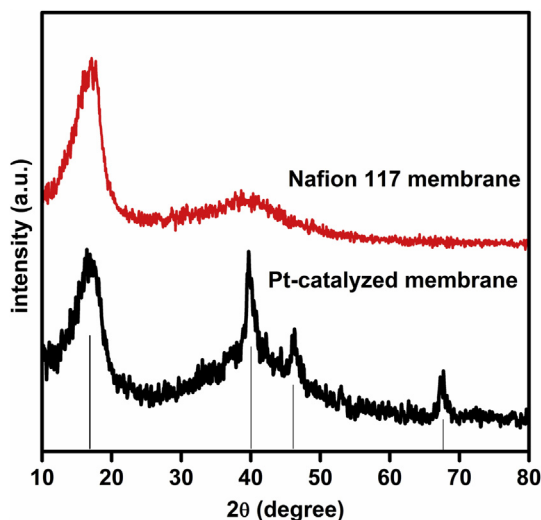
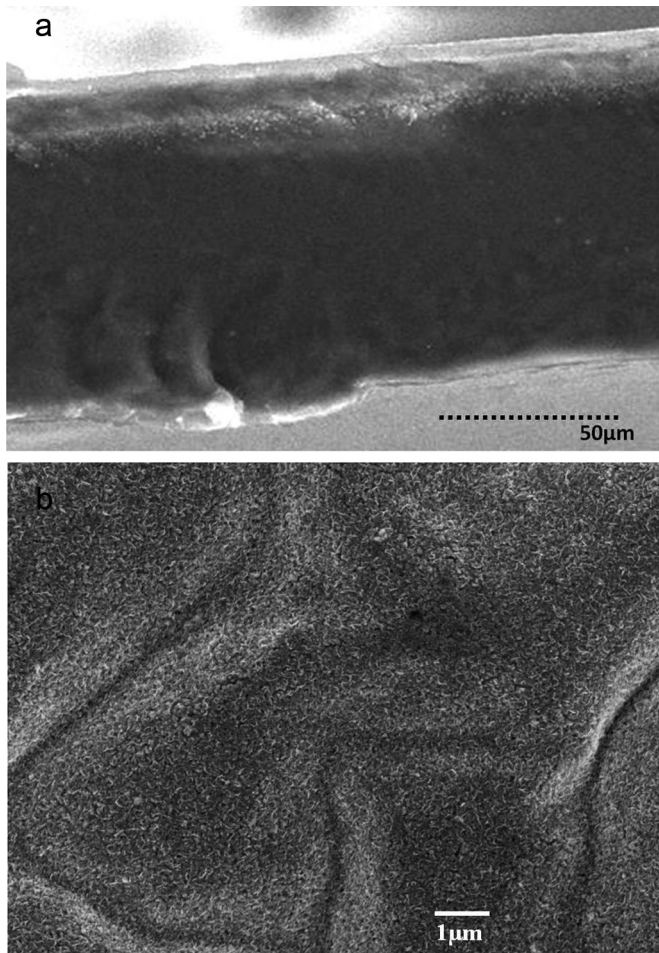
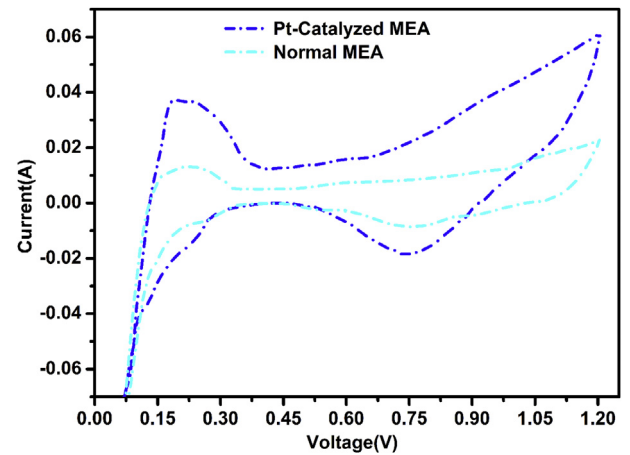


Fig. 5. X-ray diffraction pattern of Pt-catalyzed membrane and plain Nafion 117 membrane.





**Fig. 6.** a. Cross sectional HRSEM view of Pt-catalyzed membrane. b. Surface morphologies of Pt-catalyzed membrane.



**Fig. 8.** Cyclic voltammograms of Pt-catalyzed membrane electrode assembly and normal membrane electrode assembly.

membrane facilitates the three phase boundary leading to better cell performance. Because they are electrolytically connected to the Nafion membrane and electrically bound with each other's which easily enhance the three phase zone. Once the Pt-catalyzed MEA was characterized in single cell environment, the three cell stack was assembled and tested. Polarization curve, hydrogen production and long term performance of the 5 cell stack is shown in Figs. 11 and 12. From the results it is noted that the stack was able to

**Table 2**

Electrochemical properties of MEA with platinum catalyzed membrane and normal MEA.

Electrodes	Roughness factor	Electroactive surface area $\text{m}^2 \text{g}^{-1}$
Pt-catalyzed MEA membrane	230	46
Normal MEA	105	21

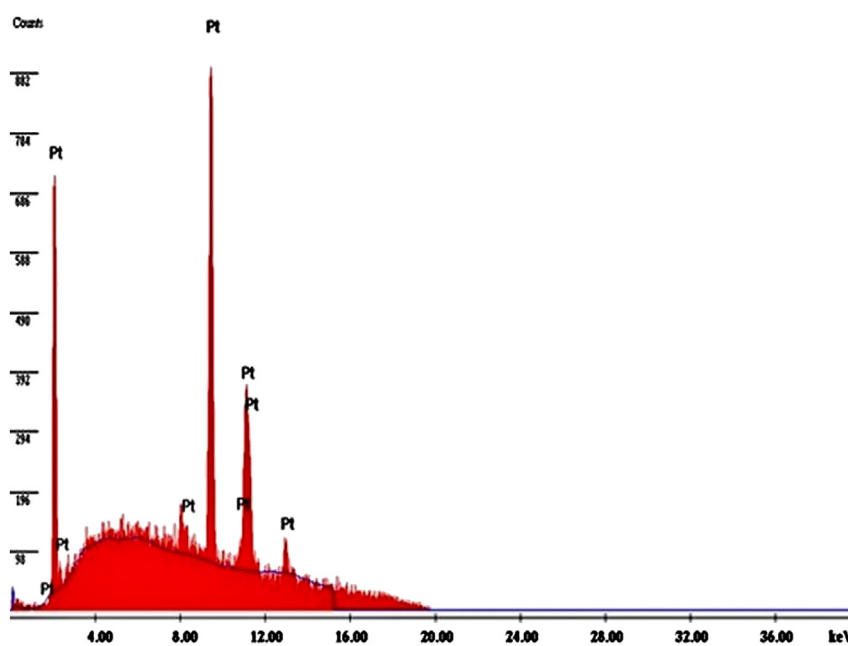


**Fig. 7.** EDX image of catalyst loaded membrane.

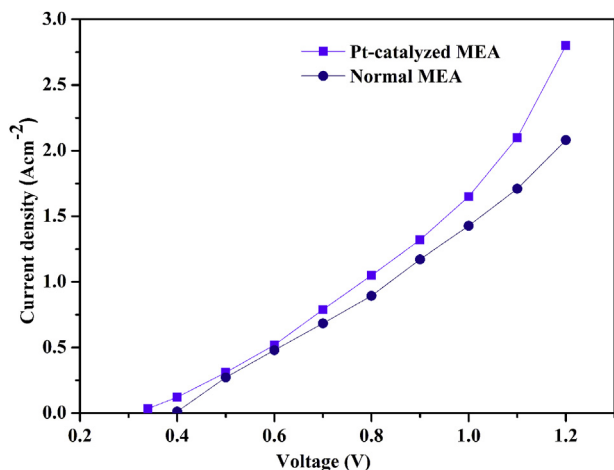


Fig. 9. Effect of operating voltage on current density of single cell.

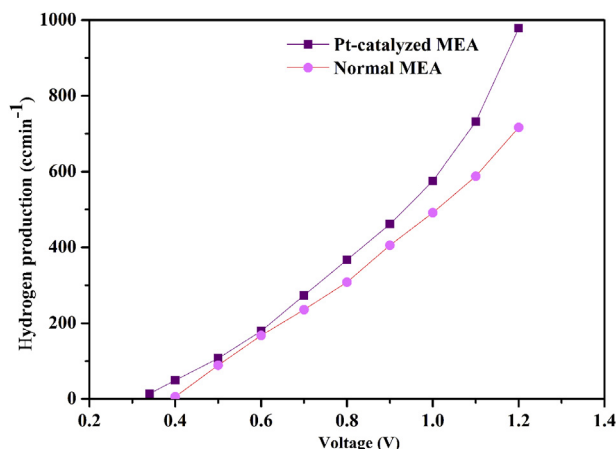


Fig. 10. Hydrogen production rate of single cell.

generate hydrogen gas about  $102 \text{ L h}^{-1}$  with 50 psi pressure at 50 A and 3.95 V. Hence, the power consumption was 197.5 W which corresponds to an energy consumption of  $1.89 \text{ kWh Nm}^{-3}$ . According to Faraday's law, the electric quantity ( $Q$ ) to produce 1 mol  $\text{H}_2$  (i.e.  $22.4 \text{ L}$  at standard condition) is  $2 \text{ F}$ . Therefore, energy consumption to produce  $1 \text{ Nm}^{-3}$  hydrogen at average single cell voltage of  $0.79 \text{ V}$  is calculated below [20],

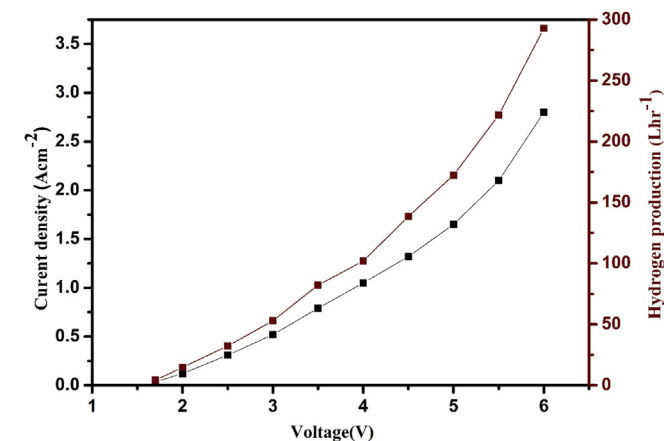


Fig. 11. Polarization curve and hydrogen production rate of methanol electrolyzer stack.

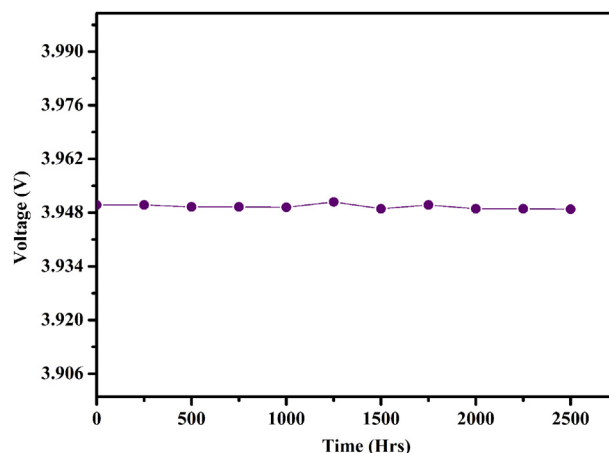


Fig. 12. Long term performance of PEM methanol electrolyzer stack operated at 50 A,  $80^\circ\text{C}$ .

$$= UIt = UQ = 0.79 \times \left(2 \times \frac{1000}{22.4} \times 96485 \times \frac{1}{1000} \times \frac{1}{3600}\right) \quad (5)$$

$$= 1.89 \text{ kWh Nm}^{-3}$$

This is very much low when compared to the energy consumption of commercial water electrolyzers ( $4.5\text{--}5 \text{ kWh Nm}^{-3}$ ) and our previous study ( $2.03 \text{ kWh Nm}^{-3}$ ) [5]. The stability of the platinum catalyzed membrane was studied at intermittent discharge rate for 2500 h Fig. 12 shows the voltage vs. time characteristics of electrolyzer under constant current density of  $1 \text{ Acm}^{-2}$  at  $80^\circ\text{C}$ . The cell voltage reached a steady state value about  $2.37 \text{ V}$  at  $1 \text{ Acm}^{-2}$ , as shown in Fig. 11. The result shows that the stability of the Pt-catalyzed membrane is excellent.

#### 4. Conclusions

In the present work, a portable PEM methanol electrolyzer with Pt-catalyzed MEA has been demonstrated and the performance was compared with normal MEA. From the results it is concluded that,

1. The developed Pt catalyzed membrane shows better performance than the normal MEA.
2. High pure hydrogen (more than 99% purity) without CO and  $\text{CO}_2$  can be obtained from PEM methanol electrolyzer, which is very much compatible for fuel cell applications. This is a major advantage compared to conventional methanol reformers.
3. Hydrogen production by electrolysis of methanol–water mixture consumes about  $1.89 \text{ kWh Nm}^{-3}$ , which is very much less than that required for water electrolysis.
4. Graphite plate with novel pore designed gas diffusion layer is used as a bipolar material and current distributors in PEM methanol electrolyzer, this is a major advantage compared to a PEM water electrolyzer, which requires costly Pt-coated titanium bipolar plate and Ti mesh current collector. Hence, the capital cost of the proposed PEM methanol electrolyzer is lower.
5. Hydrogen can be produced from a diverse array of potential feed stocks, including fossil fuels organic matter and water. Various methods are available for hydrogen production and each of these methods has its own advantages and disadvantages. Finally from the available literature review [5,21–28], we have compared the on-board and overall energy requirement for four different scenarios of hydrogen production and is shown in the table below. In the table, overall energy demand for all electrical processes is based on natural gas used in a combined cycle

power plant with 60% average efficiency in Singapore. Moreover, hydrogen from methanol scenarios, we have included energy consumption for methanol synthesized from natural gas through steam reforming. From the below information, though methanol reforming shows attractive energy consumption for on-board hydrogen production, there are several issues associated with them, such as carbon monoxide removal, long start-up time, poor transient response etc. Hence, electrolysis of methanol is a good option for producing hydrogen very quickly and conveniently. It can generate very high pure hydrogen and is considered as the most promising technology for small scale and transport applications.

Scenarios	On board energy consumption (kWh Nm <sup>-3</sup> )	Overall energy demand (kWh Nm <sup>-3</sup> )	References
Hydrogen from methane through steam reforming	2–2.5	3.33–4.17	[21–23]
Hydrogen from methanol through steam reforming	0.015–0.075	4.22–4.32	[23–26]
Hydrogen from methanol through electrolysis	1.46–2.03	6.62–7.57	[5,23,26,27]
Hydrogen from water through electrolysis	4.5–5.0	7.5–8.33	[5,23,27,28]

## References

- [1] T. Rostrup-Nielsen, Catal. Today 106 (2005) 293–296.
- [2] J.C. Amphlett, K.A.M. Creber, J.M. Davis, R.F. Mann, B.A. Peppley, D.M. Stokes, Int. J. Hydrogen Energy 19 (1994) 131–137.
- [3] J.C. Amphlett, R.F. Mann, B.A. Peppley, Int. J. Hydrogen Energy 21 (1996) 673–678.
- [4] B.A. Peppley, J.C. Amphlett, L.M. Kearns, R.F. Mann, Appl. Catal. 179 (1999) 31–49.
- [5] G. Sasikumar, A. Muthumeenal, S. Sundar Pethaiah, N. Nachiappan, R. Balaji, Int. J. Hydrogen Energy 33 (2008) 5905–5910.
- [6] R. Liu, Peter S. Fedkiw, J. Electrochem. Soc. 139 (1992) 3514–3523.
- [7] A. Katayama, A. Aramata, R. Ohnishi, J. Am. Chem. Soc. 105 (1983) 658–659.
- [8] N. Fujiwara, K. Yasuda, T. Ioroi, Z. Siroma, Y. Miyazaki, Electrochim. Acta 7 (2002) 4079–4084.
- [9] R. Liu, W.H. Her, P.S. Fedkiw, J. Electrochem. Soc. 139 (1992) 15–23.
- [10] V. Mehta, J.S. Cooper, J. Power Sources 114 (2003) 32–53.
- [11] C. Wang, Z.X. Liu, Z.Q. Mao, J.M. Xu, K.Y. Ge, Chem. Eng. J. 112 (2005) 87–91.
- [12] M.P. Godino, V.M. Barragan, J.P.G. Villaluenga, C.R. Bauza, B. Seoane, J. Power Sources 160 (2006) 181–186.
- [13] N. Rajalakshmi, H. Ryu, K.S. Dhathathreyan, Chem. Eng. J. 102 (2004) 241–247.
- [14] A. Pozio, M. De Francesco, A. Cemmi, F. Cardellini, L. Giorgi, J. Power Sources 105 (2002) 13–19.
- [15] M. Ludvigsson, J. Lindgren, J. Tegenfelt, J. Electrochem Soc. 147 (2000) 1303–1305.
- [16] F. Alcaide, G. Alvarez, J.A. Blazquez, P.L. Cabot, O. Miguel, Int. J. Hydrogen Energy 35 (2010) 5521–5527.
- [17] S. Sundar Pethaiah, G. Paruthimal Kalaighan, G. Sasikumar, M. Ulaganathan, V. Swaminathan, J. Solid State Electrochem. 17 (2013) 2917–2925.
- [18] G. Selvarani, A.K. Sahu, N.A. Choudhury, P. Sridhar, S. Pitchumani, A.K. Shukla, Electrochim. Acta 52 (2007) 4871–4877.
- [19] P. Millet, R. Durand, M. Pineri, Int. J. Hydrogen Energy 15 (1990) 245–253.
- [20] Mingyong Wang, Zhi Wang, Xuzhong Gong, Zhancheng Guo, Renewable Sustainable Energy Rev. 29 (2014) 573–588.
- [21] A.T. Raissi, D. Block, IEEE Power Energy 2 (2004) 40–45.
- [22] A. Franco, A. Russo, IJOSC 41 (2002) 843–859.
- [23] <http://sg.siemens.com/business/energy/EFossil-PAC.asp> (accessed on 03.01.14).
- [24] <http://www.caloric.com/en/produkte/h2-generation/methanol-reforming/methanol-reforming.html> (accessed on 03.01.14).
- [25] <http://www.e1na.com/pdf/e1%20H-Series%20Spec%20Sheet%20Q2%202013.pdf> (accessed on 03.01.14).
- [26] Methanol production from natural gas Angeliki A. Lemonidou, Julia Valla, Iacopos A. Vasalos, Carbon Dioxide Recovery Util. (2003) 379–394. Section VI, 2003, Springer Netherlands.
- [27] S.U.H. Jeon, T.J. Kim, J. Lee, J. Power Sources 198 (2012) 218–222.
- [28] Summary of Electrolytic Hydrogen Production, National Renewable Energy Laboratory, USA Report NREL/MP-560–36734.